1 Experimental Overview

To establish the presence of neutrino oscillation due to θ_{13}, and to determine $\sin^2 2\theta_{13}$ to a sensitivity of 0.01 or better at 90% confidence level, at least 170,000 detected events at the far site are needed, and systematic uncertainties in the ratios of near-to-far detector acceptance, antineutrino flux and background have to be controlled to a level almost an order of magnitude better than the previous experiments. Based on recent single-detector reactor experiments such as Chooz, Palo Verde and KamLAND, there are three main sources of systematic uncertainty: reactor-related uncertainty of (2–3)%, background-related uncertainty of (1–3)%, and detector-related uncertainty of (1–3)%. Each source of uncertainty can be further classified into correlated and uncorrelated uncertainties. Hence a carefully designed experiment, including the detector mass, efficiency and background control, is required. The primary considerations driving the improved performance are listed below:

- **identical near and far detectors** Use of identical antineutrino detectors at the near and far sites to cancel reactor-related systematic uncertainties, a technique first proposed by Mikaelyan et al. for the Kr2Det experiment in 1999 [1]. The event rate of the near detector will be used to predict the yield at the far detector. Even in the case of several reactors, reactor-related uncertainties can be controlled to negligible level by careful choice of the near and far site locations.

- **multiple modules** Employ multiple, identical modules at the near and far sites to cross check between modules at each location and reduce detector-related uncorrelated uncertainties. The use of multiple modules in each site enables internal consistency checks (to the limit of statistics). Multiple modules implies smaller detectors which are easier to move. In addition, small modules intercept fewer cosmic-ray muons, resulting in less dead time, less cosmogenic background and hence smaller systematic uncertainty. Taking calibration and monitoring of detectors, redundancy and cost into account, we have selected a design with two modules at each near site and four modules at the far site.

- **three-zone detector module** Each module is partitioned into three concentric zones. The innermost zone, filled with Gd-loaded liquid scintillator (Gd-LS), is the antineutrino target which is surrounded by a zone filled with unloaded LS called the γ-catcher. This middle zone is used to capture γ rays, from IBD events, that escape from the target. This arrangement can substantially reduce the systematic uncertainties related to the target volume and mass, positron energy threshold, and position cut. The outermost zone, filled with transparent mineral oil that does not scintillate, shields against external γ rays entering the active LS volume.

- **sufficient overburden and shielding** Locations of all underground detector halls are optimized to ensure sufficient overburden to reduce cosmogenic backgrounds to the level that can be measured with certainty. The antineutrino detector modules are enclosed with sufficient passive shielding to attenuate natural radiation and energetic spallation neutrons from the surrounding rocks and materials used in the experiment.

- **multiple muon detectors** By tagging incident muons, the associated cosmogenic background can be suppressed to a negligible level. This requires the muon detectors surrounding the antineutrino detectors to have a high efficiency that is known with high precision. Monte Carlo study shows that the efficiency of the muon detector should be $\geq$99.5% (with $\sigma_\epsilon \leq$0.25%). The muon system is designed to have at least two detector systems in each direction. One system utilizes the water shield as a Cherenkov detector, and another employs muon tracking detectors with decent position resolution. Each muon detector can easily be constructed with an efficiency of (90–95)% such that the overall efficiency of the muon system will be better than 99.5%. In addition, the two muon detectors can be used to measure the efficiency of each other to a uncertainty of better than 0.25%.

◦ **movable detectors** The detector modules are movable, such that swapping of modules between the near and far sites can be used to provide an even higher level of cancelation of detector-related uncertainties (to the extent that they remain unchanged before and after swapping). The residual uncertainties, being secondary, are caused by energy scale uncertainties not completely taken out by calibration, as well as other site-dependent uncertainties. The goal is to reduce the systematic uncertainties as much as possible by careful design and construction of detector modules such that swapping of detectors is not necessary. Further discussion of detector swapping will be given in Chapters **??** and **??**.

With these improvements, the total detector-related systematic uncertainty is expected to be ∼0.2% in the near-to-far ratio per detector site.

1.1 Experimental layout

Taking the current value of $\Delta m^2_{31} = 2.5 \times 10^{-3}$ eV^2 (see equation **??**), the first maximum of the oscillation associated with θ_{13} occurs at ∼1800 m. Considerations based on statistics alone will result in a somewhat shorter baseline, especially when the statistical uncertainty is larger than or comparable to the systematic uncertainty. For the Daya Bay experiment, the overburden influences the optimization since it varies along the baseline. In addition, a shorter tunnel will decrease the civil construction cost.

The Daya Bay experiment will use identical detectors at the near and far sites to cancel reactor-related systematic uncertainties, as well as part of the detector-related systematic uncertainties. The Daya Bay site currently has four cores in two groups: the Daya Bay NPP and the Ling Ao NPP. The two Ling Ao II cores will start to generate electricity in 2010–2011. Figure 1.1 shows the locations of all six cores. The

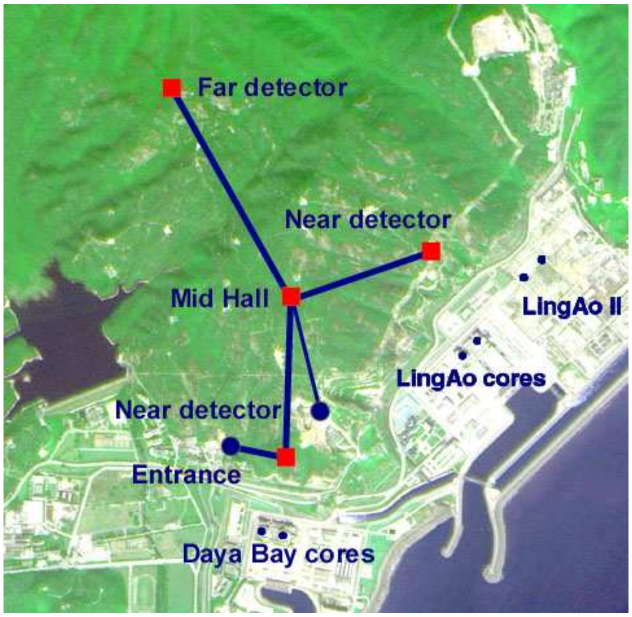

Fig. 1.1. Layout of the Daya Bay experiment.

distance between the two cores in each NPP is about 88 m. Daya Bay is 1100 m from Ling Ao, and the maximum distance between cores will be 1600 m when Ling Ao II starts operation. The experiment will locate detectors close to each reactor cluster to monitor the antineutrinos emitted from their cores as precisely as possible. At least two near sites are needed, one is primarily for monitoring the Daya Bay cores and the other primarily for monitoring the Ling Ao—Ling Ao II cores. The reactor-related systematic uncertainties can not be cancelled exactly, but can be reduced to a negligible revel, as low as 0.04% if the overburden is not taken into account. A global optimization taking all factors into account, especially balancing the overburden and reactor-related uncertainties, results in a residual reactor uncertainty of $<0.1\%$

Three major factors are involved in optimizing the locations of the near sites. The first one is overburden. The slope of the hills near the site is around 30 degrees. Hence, the overburden falls rapidly as the detector site is moved closer to the cores. The second concern is oscillation loss. The oscillation probability is appreciable even at the near sites. For example, for the near detectors placed approximately 500 m from the center of gravity of the cores, the integrated oscillation probability is $0.19 \times \sin^2 2\theta_{13}$ (computed with $\Delta m^2_{31} = 2.5 \times 10^{-3}$ eV^2). The oscillation contribution of the other pair of cores, which is around 1100 m away, has been included. The third concern is the near-far cancellation of reactor uncertainties.

After careful study of many different experimental designs, the best configuration of the experiment is shown in Fig. 1.1 together with the tunnel layout. Based on this configuration, a global χ^2 fit (see Eq. **??**) for the best sensitivity and baseline optimization was performed, taking into account backgrounds, mountain profile, detector systematics and residual reactor related uncertainties. The result is shown in Fig. 1.2.

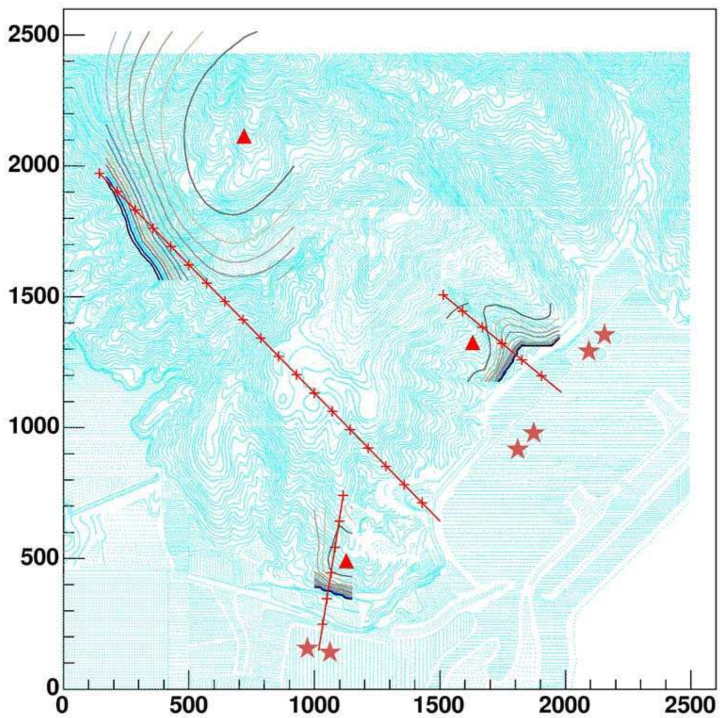

Fig. 1.2. Site optimization using the global χ^2 analysis. The optimal sites are labelled with red triangles. The stars show the reactors. The black contours show the sensitivity when one site's location is varied and the other two are fixed at optimal sites. The red lines with tick marks are the perpendicular bisectors of various combinations of reactors. The mountain contours are also shown on the plot (blue lines).

Ideally each near detector site should be positioned equidistant from the cores that it monitors so that the uncorrelated reactor uncertainties are cancelled. However, taking overburden and statistics into account while optimizing the experimental sensitivity, the Daya Bay near detector site is best located 363 m from the center of the Daya Bay cores. The overburden at this location is 98 m (255 m.w.e.).* The Ling Ao near

*The Daya Bay near detector site is about 40 m east of the perpendicular bisector of the Daya Bay two cores to gain more detector hall is optimized to be 481 m from the center of the Ling Ao cores, and 526 m from the center of the Ling Ao II cores† where the overburden is 112 m (291 m.w.e).

The far detector site is about 1.5 km north of the two near sites. Ideally the far site should be equidistant between the Daya Bay and Ling Ao—Ling Ao II cores; however, the overburden at that location would be only 200 m (520 m.w.e). At the optimized locations, the distances from the far detector to the midpoint of the Daya Bay cores and to the mid point of the Ling Ao—Ling Ao II cores are 1985 m and 1615 m, respectively. The overburden is about 350 m (910 m.w.e). A summary of the distances to each detector is provided in Table 1.1.

	DYB	LA	Far
DYB cores	363	1347	1985
LA cores	857	481	1618
LA II cores	1307	526	1613

Table 1.1. Distances (in meters) from each detector site to the centroid of each pair of reactor cores.

It is possible to install a mid detector hall between the near and far sites that is 1156 m from the midpoint of the Daya Bay cores and 873 m from the midpoint of the Ling Ao and Ling Ao II cores. The overburden at the mid hall is 208 m (540 m.w.e.). This mid hall could be used for a quick measurement of $\sin^2 2\theta_{13}$, studies of systematics and internal consistency checks.

There are three branches for the main tunnel extending from a junction near the mid hall to the near and far underground detector halls. There are also access and construction tunnels. The length of the access tunnel, from the portal to the Daya Bay near site, is 292 m. It has a grade of 9.6% [2], which allows the underground facilities to be located deeper with more overburden.

1.2 Detector Design

As discussed above, the antineutrino detector employed at the near (far) site has two (four) modules while the muon detector consists of a cosmic-ray tracking device and active water shield. There are several possible configurations for the water shield and the muon tracking detector as discussed in Section **??**. The baseline design is shown in Fig. 1.3.

The water shield in this case is a water pool, instrumented with photomultiplier tubes (PMTs) to serve as a Cherenkov detector. The outer region of the water pool is separated from the inner region by an optical barrier to provide two independent devices for detecting muons. Above the pool the muon tracking detector is made of light-weight resistive-plate chambers (RPCs). RPCs offer good performance and excellent position resolution for low cost.

The antineutrino detector modules are submerged in the water pool, shielding them from ambient radiation and spallation neutrons. Alternate water shielding configurations are discussed in Section **??**.

1.2.1 Antineutrino detector

Antineutrinos are detected by an organic LS with high hydrogen content via the inverse beta-decay reaction:

$$\bar{\nu}_e + p \longrightarrow e^+ + n$$

overburden.

†The Ling Ao near detector site is about 50 m west of the perpendicular bisector of the Ling Ao-Ling Ao II clusters to avoid installing it in a valley which is likely to be geologically weak, and to gain more overburden.

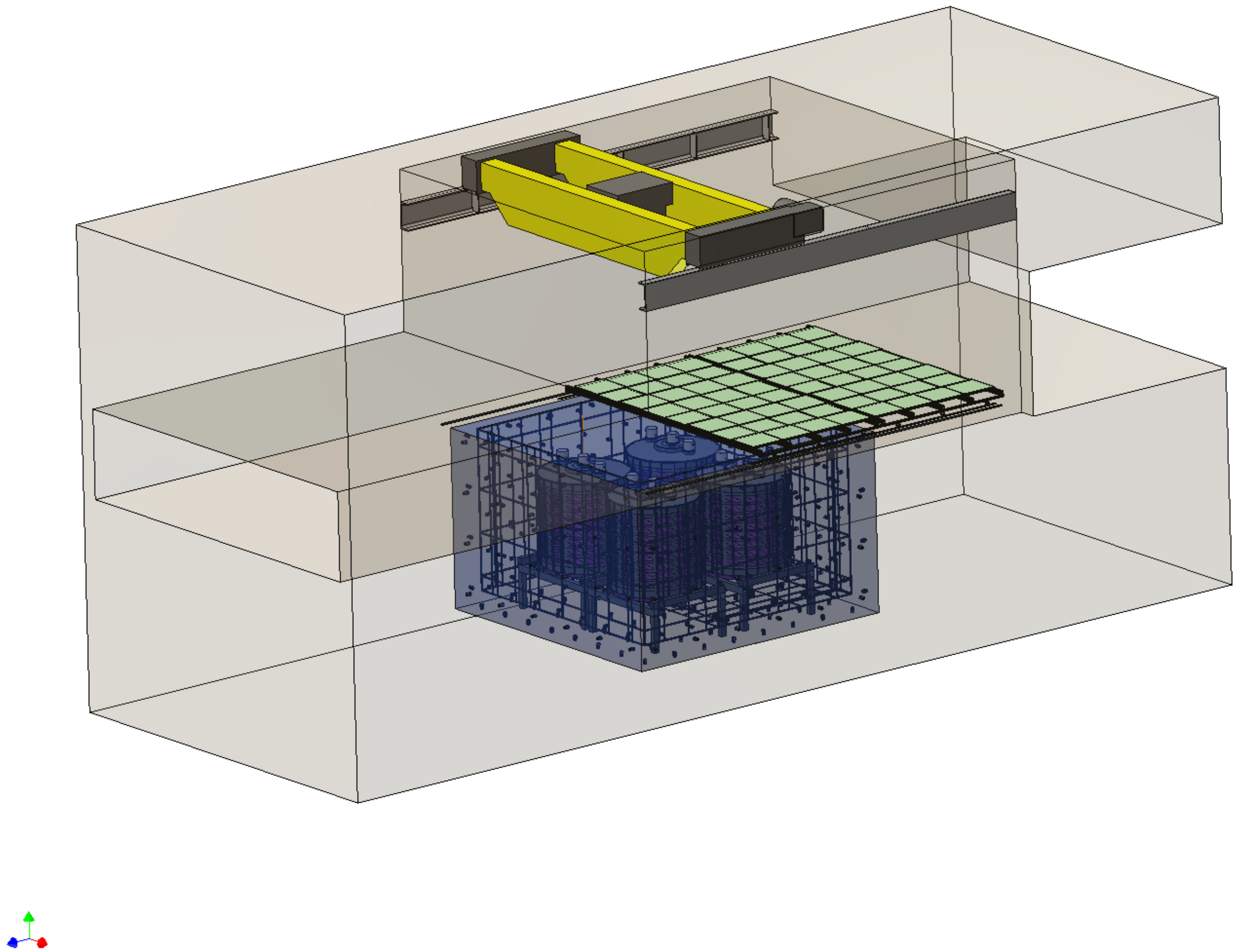

Fig. 1.3. Layout of the baseline design of the Daya Bay detector. Four antineutrino detector modules are shielded by a 1.5 m-thick active water Cherenkov shield. Surrounding this shield and optically isolated from it is another 1-meter of water Cherenkov shield. The muon system is completed with RPCs at the top.

The prompt positron signal and delayed neutron-capture signal are combined to define a neutrino event with timing and energy requirements on both signals. Neutrons are captured by hydrogen in the LS, emitting 2.2 MeV γ-rays with a capture time of 180 μs. On the other hand, when Gadolinium (Gd), with its large neutron-capture cross section and subsequent 8 MeV release of γ-ray energy, is loaded into LS the much higher γ energy cleanly separates the signal from natural radioactivity, which is mostly below 2.6 MeV, and the shorter capture time ($\sim$30 μs) reduces the background from accidental coincidences. Both Chooz [3] and Palo Verde [4] used 0.1% Gd-loaded LS that yielded a capture time of 28 μs, about a factor of seven shorter than in undoped LS. Backgrounds from random coincidences were thus reduced by a factor of seven as compared to unloaded LS.

The specifications for the design of the Daya Bay antineutrino detector modules are given as follows:

- Employ three-zone detector modules partitioned with acrylic tanks as shown in Fig. 1.4. The target

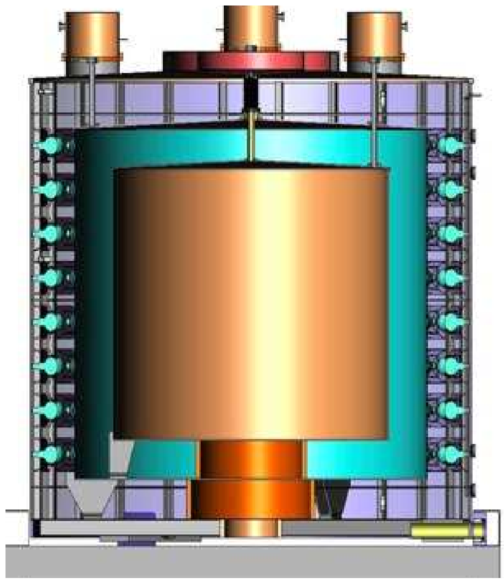

Fig. 1.4. Cross sectional slice of a 3-zone antineutrino detector module showing the acrylic vessels holding the Gd-LS at the center (20 ton), LS between the acrylic vessels (20 ton) and mineral oil (40 ton) in the outer region. The PMTs are mounted on the inside walls of the stainless steel tank.

  volume is defined by the physical dimensions of the central region of Gd-LS. This target volume is surrounded by an intermediate region filled with normal LS to catch γ rays escaping from the central region. The LS regions are embedded in a volume of mineral oil to separate the PMTs from the LS and suppress natural radioactivity from the PMT glass and other external sources.

  Four of these modules, each with 20 ton fiducial volume, will be deployed at the far site to obtain sufficient statistics and two modules will be deployed at each near site, enabling cross calibrations. Deploying an equal number of near and far detectors allows for flexibility in analyzing the data to minimize the systematic uncertainties, such as analyzing with matched near-far pairs.

  In this design, the homogeneous target volume is well determined without a position cut since neutrinos captured in the unloaded LS will not in general satisfy the neutron energy requirement. Each vessel will be carefully measured to determine its volume and each vessel will be filled with the same set of mass-flow and (volume) flow meters to minimize any variation in relative detector volume and mass. The effect of neutron spill-in and spill-out across the boundary between the two LS regions will be cancelled when pairs of identical detector modules are used at the near and far sites. With the shielding of mineral oil, the singles rate will be reduced substantially. The trigger threshold can thus be lowered to below 1.0 MeV, providing $\sim$100% detection efficiency for the prompt positron signal.

- The Gd-LS, which is the antineutrino target, should have the same composition and fraction of hydrogen for each pair of detectors (one at a near site and the other at the far site). The detectors will be filled in pairs (one near and one far detector) from a common storage vessel to assure that the composition is the same. Other detector components such as unloaded LS and PMTs will be characterized and distributed evenly to a pair of detector modules during assembly to equalize the properties of the modules.

- The energy resolution should be better than 15% at 1 MeV. Good energy resolution is desirable for reducing the energy-related systematic uncertainty on the neutron energy cut. Good energy resolution is also important for studying spectral distortion as a signature of neutrino oscillations. The primary driver for the energy resolution is to achieve sufficient energy calibration precision for neutron captures throughout the detector volume in a reasonable time.

- The time resolution should be better than 1 ns for determining the event time and for studying backgrounds.

Detector modules of different shapes, including cubical, cylindrical, and spherical, have been considered. From the point of view of ease of construction cubical and cylindrical shapes are particularly attractive. Monte Carlo simulation shows that modules of cylindrical shape can provide better energy and position resolutions for the same number of PMTs. Figure 1.4 shows the structure of a cylindrical module. The PMTs are arranged along the circumference of the outer cylinder. The surfaces at the top and the bottom of the outer-most cylinder are coated with diffuse reflective materials. Such an arrangement is feasible since 1) the event vertex is determined only with the center of gravity of the charge, not relying on the time-of-flight information,[‡] 2) the fiducial volume is well defined with a three-zone structure, thus no accurate vertex information is required. Details of the antineutrino detector will be discussed in Chapter **??**.

1.2.2 Muon detector

Since most backgrounds originate from cosmic-ray muon interactions with nearby materials, it is desirable to have a very efficient muon detector with some tracking capability. This enables the study and rejection of cosmogenic backgrounds. The two detector technologies are water Cherenkov counters and RPCs. The combined water Cherenkov detector and RPC can achieve muon detection efficiencies close to 100%. Furthermore, these two independent detectors can cross check each other. Their inefficiencies and the associated uncertainties can be well determined by cross calibration during data taking. We expect the inefficiency will be lower than 0.5% and the uncertainty of the inefficiency will be better than 0.25%.

Besides being a shield against ambient radiation, the water shield can also be utilized as a water Cherenkov counter by installing PMTs in the water. The water Cherenkov detector is based on proven technology, and known to be very reliable. With sufficient PMT coverage and reflective surfaces, the efficiency of detecting muons should exceed 95%. The current baseline design of the water shield is a water pool, similar to a swimming pool with a dimensions of 16 m (length) $\times$ 16 m (width) $\times$ 10 m (height) for the far hall containing four detector modules, as shown in Fig. 1.5. The PMTs of the water Cherenkov counters are mounted facing the inside of each water volume. This is a simple and proven technology with very limited safety concerns. The water will effectively shield the antineutrino detectors from radioactivity in the surrounding rocks and from radon, with the attractive features of being simple, cost-effective and rapidly deployable.

RPCs are very economical for instrumenting large areas, and simple to fabricate. The Bakelite based RPC developed by IHEP for the BES-III detector has a typical efficiency of 95% and noise rate of 0.1 Hz/cm^2 per layer [5]. A possible configuration is to build four layers of RPC, and require three out of four layers hit within a time window of 20 ns to define a muon event. Such a scheme has an efficiency and low noise rate. Although RPCs are an ideal large area muon detector due to their light weight, good performance, excellent position resolution and low cost, it is hard to put them inside water to fully surround the water pool. The best choice seems to use them only at the top of the water pool.

[‡]Although time information may not be used in reconstructing the event vertex, it will be used in background studies. A time resolution of 0.5 ns can be easily realized in the readout electronics.

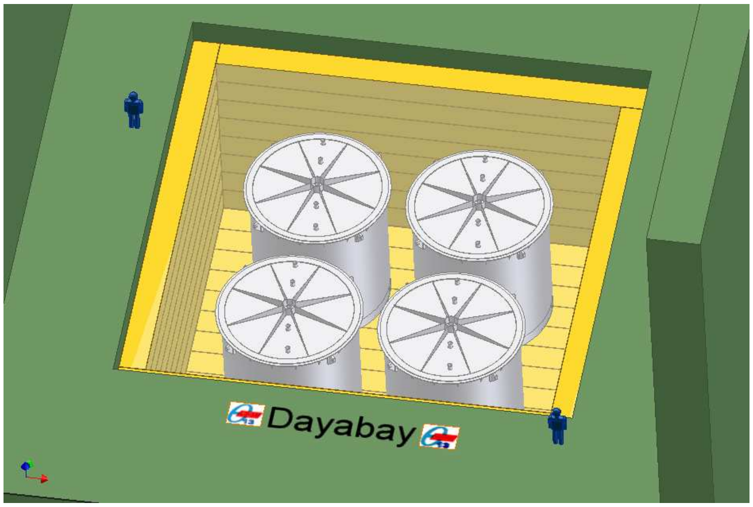

Fig. 1.5. The water pool with four antineutrino detector modules inside.

REFERENCES

1. L.A. Mikaelyan and V. V. Sinev, Phys. Atom. Nucl. **63**, 1002 (2000); L. Mikaelyan, Nucl. Phys. Proc. Suppl. **91**, 120 (2001); L.A. Mikaelyan, Phys. Atom. Nucl. **65**, 1173 (2002).
2. *Report of Preliminary Feasibility Study of Site Selection for the Daya Bay Neutrino Experiment*, prepared by Beijing Institute of Nuclear Energy, September, 2004.
3. M. Apollonio *et al*. (Chooz Collaboration), Phys. Lett. B**420**, 397 (1998); Phys. Lett. **B466**, 415 (1999); Eur. Phys. J. C**27**, 331 (2003).
4. F. Boehm *et al.* (Palo Verde Collaboration), Phys. Rev. Lett. **84**, 3764 (2000) [arXiv:hep-ex/9912050]; Phys. Rev. D**62**, 072002 (2000) [arXiv:hep-ex/0003022]; Phys. Rev. D**64**, 112001 (2001) [arXiv:hep-ex/0107009]; A. Piepke et al., Nucl. Instr. and Meth. **A432**, 392 (1999).
5. J.W. Zhang *et al.*, High Energy Phys. and Nucl. Phys., **27**, 615 (2003); JiaWen Zhang et al., Nucl. Inst. Meth. **A540**, 102 (2005).